46th AIAA/ASME/SAE/ASEE Joint Propulsion Conference & Exhibit
25 - 28 July 2010, Nashville, TN

AIAA 2010-6615



# The Influence of Induced Currents on Magnetic Nozzle Acceleration and Plasma Detachment

Justin M. Little * and Edgar Y. Choueiri †

*Electric Propulsion and Plasma Dynamics Laboratory*

*Princeton University, Princeton, NJ, 08544*

**The influence of induced currents on the acceleration and detachment of a uniform plasma expanding through a magnetic nozzle is investigated. A collisionless two-fluid model is used to solve for the flow of a cold-ion, hot-electron plasma through a diverging magnetic field. An iterative procedure is then employed to converge upon a magnetic field solution consistent with the plasma dynamics. The ratio of the kinetic energy density to the magnetic field energy density at the nozzle throat, $\beta_0$, is found to control the relative importance of induced currents within the flow while the acceleration of the plasma is largely independent of $\beta_0$. The efficiency at which the plasma detaches from the magnetic nozzle, on the other hand, increases with $\beta_0$ due to the influence of induced magnetic fields on the plume divergence. Finally, it is concluded that the predominant physical mechanism behind plasma detachment is the inertial separation of the flow from the magnetic field as the electron Larmor radius increases beyond the scale length of magnetic field variation. The local value of $\beta$ at the detachment location reflects the relative importance of induced currents on plasma detachment.**



## Nomenclature

| | |
|---|---|
| $\vec{B}$ | Magnetic field |
| $\Psi$ | Magnetic flux function |
| $a$ | Applied field coil radius |
| $\gamma$ | Specific heat ratio |
| $r_L$ | Larmor radius |
| $G$ | Inertial detachment parameter |
| $\beta_0$ | Plasma $\beta$ at nozzle entrance |
| $\epsilon_{avg}$ | Average error for magnetic solver |
| $W_{th}$ | Work due to thermal forces |
| $W_{em}$ | Work due to electromagnetic forces |
| $\eta_{nozzle}$ | Overall nozzle efficiency |
| $\eta_{max}$ | Maximum nozzle efficiency |
| $\eta_{acc}$ | Acceleration efficiency |
| $\eta_{div}$ | Divergence efficiency |
| $P_{thrust}$ | Directed kinetic power of the flow |
| $P_{in}$ | Total incoming power within the flow |
| $P_{ke}$ | Total kinetic power of the flow |
| $u_{ci}$ | Critical ionization velocity |
| $\epsilon_i^+$ | Ionization energy |
| $Th$ | Thrust |
| $I_{sp}$ | Specific impulse |
| $\xi_{mag}$ | Electron magnetization parameter |

*Graduate Research Assistant

†Chief Scientist, EPPDyL; Professor, Applied Physics Group, Mechanical and Aerospace Engineering Department; AIAA Fellow.

# I. Introduction

A number of plasma propulsion concepts currently being investigated rely on the use of applied magnetic fields to accelerate heated plasmas to exhaust velocities an order of magnitude larger than chemical rockets.[1,2] In a process akin to conventional de Laval nozzles, these "magnetic nozzles" use a converging-diverging magnetic field to convert the thermal energy of a plasma into directed kinetic energy while simultaneously preventing the energetic plasma from impacting the surfaces of the thruster.[3] The feasibility of using plasma flow along magnetic fields to produce thrust has been questioned, however, due to the tendency of plasma to remain tied to necessarily closed magnetic field lines. Efficient detachment of the plasma from the magnetic nozzle thus becomes paramount for the potential application of such concepts to space propulsion.

Several physical mechanisms have been proposed to describe plasma detachment from magnetic nozzles. These mechanisms can be divided into two general categories: collisional and collisionless detachment.

Collisional detachment encompasses both resistive diffusion of the plasma across the applied magnetic field[4] and detachment through three-body recombination of the ionized propellant into neutral particles.[5] Both of these processes are sensitive to their respective collision frequencies, which depend upon the evolution of the electron temperature in the nozzle plume. Experimental and computational studies suggest that the distance over which electron cooling occurs within the expanding plasma is insufficient to allow for significant amounts of cross-field diffusion or three-body recombination.[6–8]

Plasma detachment may occur in the collisionless limit due to either inertial separation of the plasma from the magnetic field[9–11] or stretching of the magnetic field along with the flow.[12–15] Using a two-fluid model of a cold plasma expanding through a dipole magnetic field, Hooper demonstrated that detachment is theoretically possible due to the finite inertia of the flowing plasma. He finds inertial plasma detachment is dependent on a parameter which is inversely proportional to the product of the electron and ion Larmor radii. In essence, Hooper's inertial detachment parameter, $G$, is a ratio of the effective magnetic field inertia to the plasma inertia. However, by ignoring induced magnetic fields, Hooper's analysis is limited to low-$\beta$ plasmas where $\beta$ is defined as the ratio of the kinetic energy of the flow to the the energy stored within the magnetic fields of the nozzle. Arefiev and Breizman used magnetohydrodynamics[12,13] to show that the magnetic fields of the nozzle are stretched along the flow by an induced azimuthal current density that develops within the plasma as $\beta$ increases beyond unity. However, this theoretical framework is limited to "frozen-in" flow from which the plasma fluid elements cannot strictly detach from the magnetic field. Furthermore, the physical source of the induced current density is unclear from their analysis.

While separate studies have been done of inertial detachment of plasma from static magnetic fields and the effect of induced currents in magnetic nozzle plumes, there has yet to be a comprehensive investigation that encompasses both of these related phenomena. The following questions thus arise: *under what conditions do induced currents in magnetic nozzle plumes affect plasma detachment?* And, more importantly, *how do induced currents physically influence the accelerating plasma and the efficiency at which it detaches from the magnetic nozzle?* It is mainly the later question that we address in this paper.

Using a two-fluid model for plasma expansion with a consistent magnetic field solution, we show that the inertial separation of plasma elements from surfaces of constant magnetic flux produces an azimuthal current density that acts to stretch the magnetic field along with the flow. The degree to which this field stretching occurs is strongly dependent on the inertial detachment parameter, $G$, the ratio of the incoming plasma radius to the magnetic coil radius, $\hat{r}_{p,0}$, and the value of $\beta$ at the throat, $\beta_0$. While keeping $G$ and $\hat{r}_{p,0}$ constant, we present solutions for two cases: a "low-$\beta$" flow and a "moderate-$\beta$" flow. We compare the physical properties and resulting propulsion efficiencies of each flow to determine the extent to which induced currents affect plasma expansion through magnetic nozzles. Finally, our analysis concludes with an investigation of the predominant detachment mechanism for each flow.

# II. Plasma Detachment Model

An investigation of the influence that induced currents have on expanding magnetic nozzle plasmas requires a consistent description of the magnetic field within the flow. In light of this requirement, we have developed a two-fluid model for the expansion of a cold-ion, hot-electron plasma through an applied dipole magnetic field, for which an iterative procedure is used to converge upon a magnetic field solution consistent with the dynamics of the plasma flow. A depiction of our model may be seen in Figure 1.

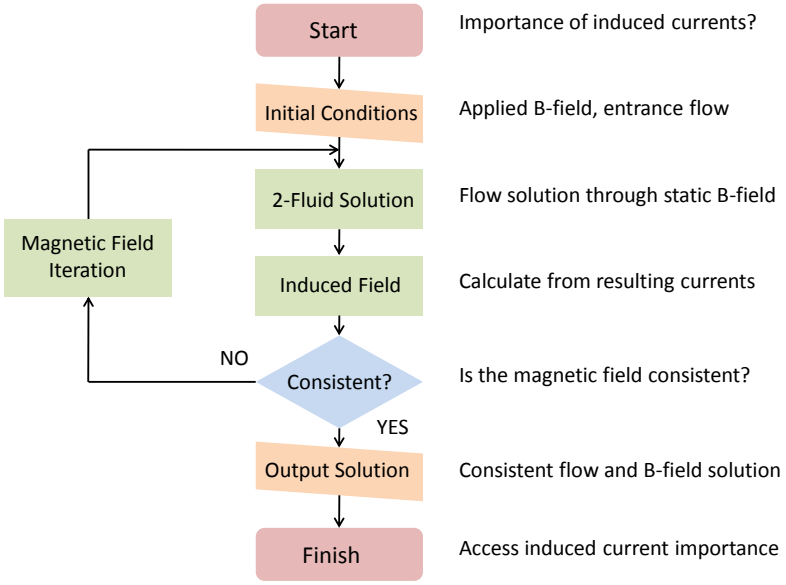


**Figure 1. Flow chart describing the iterative scheme used to converge on a solution for magnetic nozzle flow with a consistent magnetic field.**



### II.A. Applied Magnetic Field

The axisymmetric nature of a magnetic nozzle permits the description of its applied magnetic field, $B_N$, in terms of a scalar flux function, $\Psi_N$,

$$\vec{B}_N = \frac{1}{r}\left(\hat{e}_\theta \times \vec{\nabla}\Psi_N\right) = -\frac{1}{r}\frac{\partial \Psi_N}{\partial z}\hat{e}_r + \frac{1}{r}\frac{\partial \Psi_N}{\partial r}\hat{e}_z, \tag{1}$$

where, $\langle \hat{e}_z, \hat{e}_r, \hat{e}_\theta \rangle$ represent the unit vectors in cylindrical coordinates.

Modeling our applied magnetic field as that due to a single loop of current with radius $a$ centered at the origin yields the following form for $\Psi_N$,

$$\Psi_N = \frac{2B_0 a^2 r}{\pi}\frac{\left(2-k^2\right)K\left(k^2\right) - 2E\left(k^2\right)}{k^2\sqrt{(a+r)^2+z^2}}, \tag{2}$$

where

$$k^2 = \frac{4ra}{(r+a)^2+z^2}, \tag{3}$$

and $K$ and $E$ represent complete elliptic integrals of the first and second kind, respectively.[16]

### II.B. Plasma Expansion

The acceleration and expansion of plasma through a diverging magnetic field has been previously investigated numerous times using models of varying complexity.[9,10,13,17–20] Lacking from this literature is a simple model that allows simultaneously for thermal acceleration, induced magnetic fields, and inertial separation of the plasma from the magnetic field lines. It is these three properties of magnetic nozzle expansion that our model aims to capture.

We begin by solving for the dynamics of a uniform plasma flow through the throat of a static magnetic field using a Lagrangian specification for a two-fluid flow. Later, we will calculate the induced magnetic field and iterate upon the static magnetic field (sections II.D. and II.E.). Neglecting collisions, the conservation

of momentum, continuity, and energy for each species take the following form:

$$m_s n_s \left(\vec{u}_s \cdot \vec{\nabla}\right) \vec{u}_s = q_s n_s \left(\vec{E} + \vec{u}_s \times \vec{B}\right) - \vec{\nabla} p_s, \tag{4}$$

$$\vec{\nabla} \cdot (n_s \vec{u}_s) = 0, \tag{5}$$

$$\frac{d}{dt}\left(\frac{p_s}{n_s^{\gamma_s}}\right) = 0, \tag{6}$$

where the subscript $s$ denotes the species.

Furthermore, we assume the plasma is fully ionized ($n_n = 0$), quasineutral ($n_e = n_i = n_0$), and that local ambipolarity holds throughout the entire plume ($u_{r,i} = u_{r,e}, u_{z,i} = u_{z,e}$). Finally, we consider the flow of cold ions ($T_i = 0$) for which acceleration occurs as the electron thermal energy is converted into ion kinetic energy by the ambipolar electric field.

Non-dimensionalizing the system of equations and following a similar procedure as that of Hooper, we arrive at the following equations describing the plasma dynamics of the expanding plume:

$$\hat{u}_{\theta,s} = \frac{1}{\hat{r}_{Ls,0}}\left(\frac{\hat{\Psi}_0 - \hat{\Psi}}{\hat{r}}\right), \tag{7}$$

$$\frac{d\hat{u}_z}{d\hat{t}} = -\frac{1}{\hat{n}}\left(\frac{\hat{n}}{\hat{n}_0}\right)^{\gamma-1}\frac{\partial \hat{n}}{\partial \hat{z}} - G\frac{\partial}{\partial \hat{z}}\left[\frac{(\hat{\Psi}_0 - \hat{\Psi})^2}{2\hat{r}^2}\right], \tag{8}$$

$$\frac{d\hat{u}_r}{d\hat{t}} = -\frac{1}{\hat{n}}\left(\frac{\hat{n}}{\hat{n}_0}\right)^{\gamma-1}\frac{\partial \hat{n}}{\partial \hat{r}} - G\frac{\partial}{\partial \hat{r}}\left[\frac{(\hat{\Psi}_0 - \hat{\Psi})^2}{2\hat{r}^2}\right], \tag{9}$$

$$\frac{d\hat{z}}{d\hat{t}} = \hat{u}_z, \tag{10}$$

$$\frac{d\hat{r}}{d\hat{t}} = \hat{u}_r. \tag{11}$$

Here, $\hat{r}_{Ls,0}$ is the normalized Larmor radius of species $s$ at the throat, $\hat{\Psi}_0$ is the normalized flux function value of the fluid element at the throat, $\hat{\Psi}$ is the local value of the normalized flux function, $G$ is Hooper's inertial detachment parameter, defined as

$$G = \frac{a^2 e^2 B_0^2}{m_e M_i c_{si,0}^2} = \frac{1}{\hat{r}_{Li,0}\hat{r}_{Le,0}}, \tag{12}$$

and the non-dimensional parameters are given by

$$\hat{u}_z = \frac{u_z}{c_{s,0}} \qquad \hat{u}_r = \frac{u_r}{c_{s,0}} \qquad \hat{u}_\theta = \frac{u_\theta}{c_{s,0}} \qquad \hat{t} = \frac{t c_{s,0}}{a} \qquad \hat{z} = \frac{z}{a} \qquad \hat{r} = \frac{r}{a} \tag{13}$$

$$\hat{\Psi} = \frac{\Psi}{B_0 a^2} \qquad \hat{j}_\theta = \frac{a j_\theta \mu_0}{B_0} \qquad \hat{n} = n\frac{\mu_0 a e c_{s,0}}{B_0}, \tag{14}$$

where we have used the speed of sound at the throat, $c_{s,0}$, magnetic field at the origin, $B_0$, and nozzle radius, $a$, to normalize the variables of our system of equations.

### II.C. Quasi-One-Dimensional Pressure

The most accurate description of the expanding plasma under the stated assumptions requires the simultaneous solution of Equations (8)-(11) along with the continuity equation. Previous models[19,20] investigating the acceleration of magnetic nozzle plasmas have followed this procedure, however, plasma detachment was impossible as it was required that the electron motion remain tied to the magnetic field lines for prior knowledge of the plume boundary. With the desire to solve the problem in a much simpler Lagrangian reference frame, we look for a pressure model in terms of only local variables along a given streamline.

Assuming most of the acceleration happens within a few nozzle radii of the throat, the streamlines of the flow in the acceleration region are taken to be approximately aligned with lines of constant magnetic

flux. Using a tilde notation to denote the projection of a vector onto the meridional $(r-z)$ plane, this approximation allows us to write

$$\tilde{u}\cdot\tilde{\nabla}\left(\frac{nu_{\parallel}}{B}\right)\approx 0, \tag{15}$$

with the density along a streamline given by

$$\frac{\hat{n}}{\hat{n}_0}\approx\frac{\hat{B}}{\hat{u}_{\parallel}}. \tag{16}$$

Here, $\hat{u}_{\parallel}$ is the magnitude of the velocity projected onto the magnetic field line. Finally, assuming the flow remains slowly divergent and that the density gradient in the radial direction is much less than the axial direction ($\partial\hat{n}/\partial\hat{z} >> \partial\hat{n}/\partial\hat{r}\approx 0$), we may approximate the parallel velocity as

$$u_{\parallel}\approx u_z+\frac{u_r^2}{2u_z}, \tag{17}$$

and combine this expression with Eq.(12) to yield the following equation for the axial variation of the density in terms of only local variables,

$$\frac{1}{\hat{n}}\frac{\partial\hat{n}}{\partial\hat{z}}\approx-\frac{1}{\hat{u}_z^2}\frac{\left(2\hat{u}_z^2-\hat{u}_r^2\right)}{\left(2\hat{u}_z^2+\hat{u}_r^2\right)}\frac{d\hat{u}_z}{d\hat{t}}-\frac{1}{\hat{u}_z\hat{u}_r}\frac{2\hat{u}_r^2}{\left(2\hat{u}_z^2+\hat{u}_r^2\right)}\frac{d\hat{u}_r}{d\hat{t}}+\frac{1}{\hat{B}}\frac{\partial\hat{B}}{\partial\hat{z}}+\frac{\hat{u}_r}{\hat{u}_z\hat{B}}\frac{\partial\hat{B}}{\partial\hat{z}}. \tag{18}$$

Therefore, combining Eq.(18) with Eqs.(8)-(11) allows us to solve for the evolution of the position and velocity of a fluid element given its position and velocity at the nozzle throat.

### II.D. Induced Magnetic Field

Equation (4) indicates the dependence of the azimuthal velocity of each species on the inverse of their initial Larmor radius at the throat. The result of this dependence is an electron azimuthal velocity greater than that of the ions by the ratio of their masses: a result which creates a net current in the azimuthal direction. Considering only the electron current, Equations (7) and (14) yield the following expression for the azimuthal current along a given streamline,

$$\hat{j}_{\theta}=G\beta_0\frac{\hat{n}}{\hat{n}_0}\left(\frac{\hat{\Psi}_0-\hat{\Psi}}{\hat{r}}\right), \tag{19}$$

where

$$\beta_0=\frac{n_0m_ic_{si,0}^2}{B_0^2/\mu_0}, \tag{20}$$

is the ratio of the incoming kinetic energy density of the plasma to the energy density stored within the magnetic field at the nozzle throat. Therefore, it is seen that the formation of azimuthal currents within the nozzle plume is due to separation of the plasma from its initial flux line, $\hat{\Psi}_0-\hat{\Psi}$, and is dependent on both of the dimensionless parameters associated with previous plasma detachment theories, $G$ and $\beta_0$. It is thus reasonable to suspect that a balance may exist between the propensity of the plasma to separate from the magnetic field due to its inertia and the tendency of the magnetic field to be pulled along with the plasma.

By solving for the current density along multiple streamlines, we construct a current density distribution within the plasma. We then take the dimensionless induction equation,

$$\hat{\nabla}\times\hat{B}=\hat{j}_{\theta}\hat{e}_{\theta}, \tag{21}$$

and recast it as an elliptic partial differential equation in terms of the induced flux function, $\hat{\Psi}_i$.

$$\frac{1}{\hat{r}}\hat{\nabla}^2\hat{\Psi}_i-\frac{1}{\hat{r}^2}\frac{\partial\hat{\Psi}_i}{\partial\hat{r}}=\hat{j}_{\theta}. \tag{22}$$

Finally, we numerically solve the above equation for $\hat{\Psi}_i$ using a finite differencing scheme that incorporates both Gauss-Seidel iteration and Von-Hagenow's method for calculating boundary conditions.[21] Figure 2(a) shows surfaces of constant $\hat{\Psi}_i$ obtained from the numerical solution to Equation (22) for a single loop of current with radius $r=1$ located at $z=1$. A comparison between the numerical solution and the analytic solution along the line $z=1$ shows good agreement (Figure 2(b)).

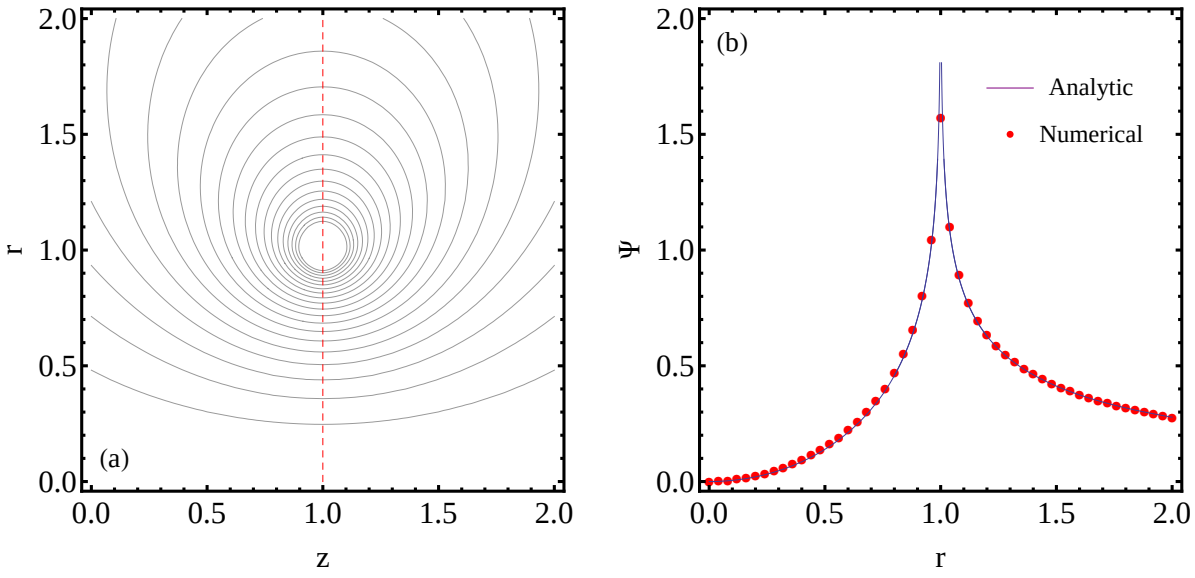


**Figure 2. Benchmark solution for magnetic field solver. (a) Numerical solutions for lines of constant magnetic flux, $\Psi$, for a single loop of current placed at $r = 1, z = 1$. (b) Comparison of the numerical solution with the analytic solution for the magnetic flux along the vertical line at $z = 1$.**



### II.E. Iteration Scheme

The total magnetic field is given by the sum of the applied magnetic field and the induced magnetic field, which may be expressed as

$$\hat{\Psi}_0 = \hat{\Psi}_N + \hat{\Psi}_i. \tag{23}$$

However, consistency with the dynamics of the flow requires that the total flux function input to the two-fluid model be equal to the applied flux function plus the resulting induced flux function. We use the average error, $\epsilon_{avg}$, between the input and output flux functions as a measure of consistency, where

$$\epsilon_{avg} = \frac{1}{n^2} \sum_{j=1}^{n} \sum_{k=1}^{n} \left| 1 - \frac{\hat{\Psi}_0^{(in)}(z_j, r_k)}{\hat{\Psi}_0^{(out)}(z_j, r_k)} \right|. \tag{24}$$

If the average error is greater than a threshold value (typically $10^{-4}$), the input flux function is iterated upon using the output flux function of the previous iteration until $\epsilon_{avg}$ decreases below the threshold. Using this method, consistent solutions for plasmas with $\beta \leq 10^{-3}$ have been obtained. The initial output flux function for plasmas with $\beta > 10^{-3}$ is too large for this iteration scheme to work in its current form.

## III. Results

Assuming the flow through the nozzle to be choked ($\hat{u}_{z,0} \approx 1$), four dimensionless parameters defined at the throat uniquely determine the solution to our model: the inertial detachment parameter, $G$, the ratio of the flow energy density to the magnetic field energy density, $\beta_0$, the ratio of the plasma radius to the applied field coil radius, $\hat{r}_{p,0}$, and the electron ratio of specific heats, $\gamma$. To investigate the influence of induced currents on the resulting plasma flow, we consider a "low-$\beta$" flow ($\beta_0 = 10^{-5}$) and a "moderate-$\beta$" flow ($\beta_0 = 10^{-3}$). A normalized plasma radius of $\hat{r}_{p,0} = 0.18$ is used along with a value of $G = 4 \times 10^5$ and $\gamma = 1.2$ for both cases. These parameters are representative of a typical Argon plasma flow through a compact helicon thruster with $T_{e,0} \approx 40eV$, $a \approx 0.1m$, and $B_0 \approx 0.1T$.[22]

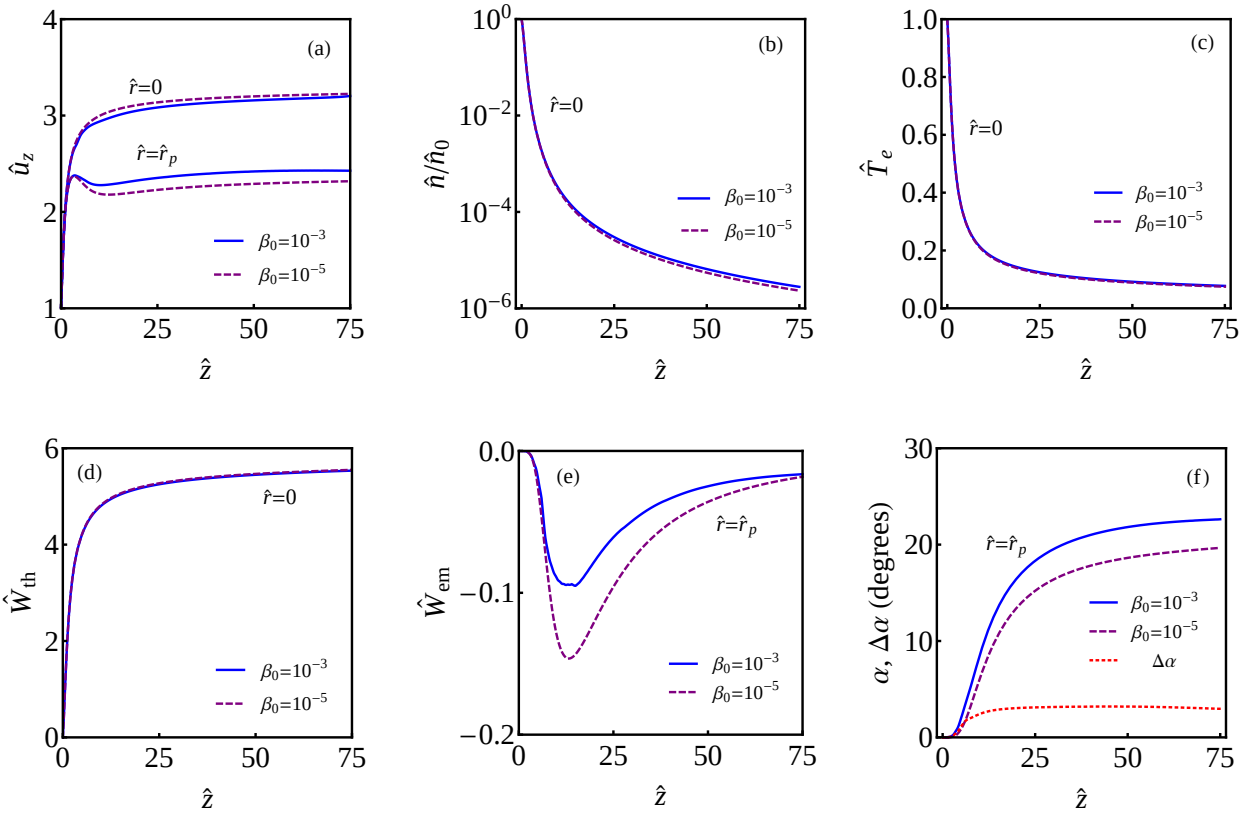


**Figure 3. Axial variation for $\beta_0 = 10^{-5}$ (dashed) and $\beta_0 = 10^{-3}$ (dotted) of: (a) axial velocity, (b) density relative to entrance density, (c) electron temperature, (d) thermal work, (e) electromagnetic work, and (f) angle of separation and relative separation. Results for each $\beta_0$ are found for $G = 4 \times 10^5$ and $\hat{r}_{p,0} = 0.18$.**

### III.A. Expansion Properties

The evolution throughout the plume of the axial velocity, density, and electron temperature along a given streamline is presented in Figures 3(a)-3(c). The axial velocity is shown for both the streamline corresponding to the nozzle axis ($\hat{r} = 0$) and the streamline corresponding the plume edge ($\hat{r} = \hat{r}_p$). It can be seen that most of the acceleration occurs within five nozzle radii of the throat. Furthermore, a decrease in axial velocity is observed along the outermost streamline, for which the moderate-$\beta$ flow shows a smaller decrease than the low-$\beta$ flow. Figure 3(b) indicates a similar density profile for both flows, however, the density falls off slightly faster for the low-$\beta$-flow. The decrease in electron temperature, shown in figure 3(c), shows little dependence on the value of $\beta_0$.

To help understand the dynamics of the expanding plasma for each case, we consider the work done by thermal and electromagnetic forces on a fluid element as it escapes the nozzle. Normalizing the work due to each force by the electron temperature at the nozzle throat, we arrive at the following expressions:

$$\hat{W}_{th} = \frac{\gamma}{\gamma - 1}\left[1 - \left(\frac{\hat{n}}{\hat{n}_0}\right)^{\gamma-1}\right], \tag{25}$$

$$\hat{W}_{em} = -\gamma G\left[\frac{(\hat{\Psi}_0 - \hat{\Psi})^2}{\hat{r}^2}\right]. \tag{26}$$

Here, we denote $\hat{W}_{th}$ as the work due to thermal forces and $\hat{W}_{em}$ as that due to electromagnetic forces. We should note that some ambiguity exists between the actual sources of this work as the thermal work results from a relationship between the ambipolar electric field and electron pressure. Furthermore, the electromagnetic work is due to a combination of the magnetic ($\vec{u} \times \vec{B}$) force, which technically does no work

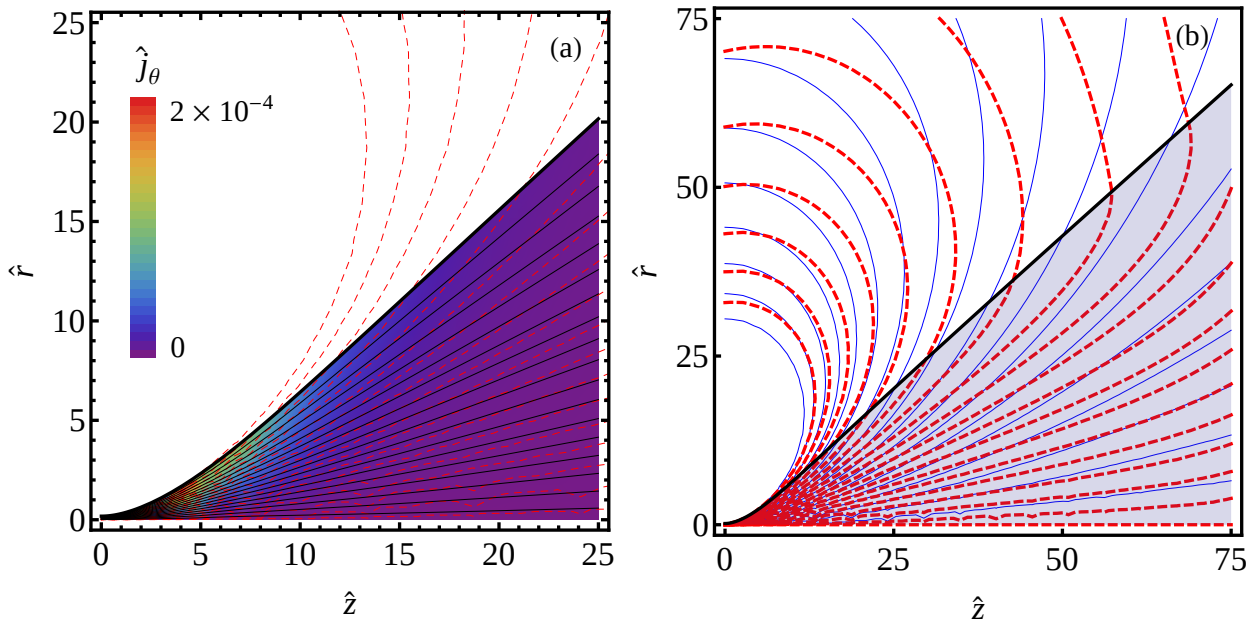


**Figure 4. Results for the $\beta_0 = 10^{-3}$ flow for: (a) current density distribution with streamlines (solid black) and magnetic flux lines (dashed red), and (b) comparison between applied magnetic flux lines (solid blue) and resulting magnetic flux lines (dashed red).**

on the particles, and the centrifugal force. However, Eq. 26 represents the work due to the projection of these forces on the meridional plane, and is in essence a measure of how much energy has been deposited into the rotation of the plasma.

Figures 3(d)-3(e) show the thermal work along the nozzle axis, and the electromagnetic work along the plume edge, respectively. The thermal work for each flow is nearly identical, which suggests that induced field effects have a negligible role on the thermal acceleration of the plasma. The work due to electromagnetic forces is seen to decrease rapidly then increase towards an asymptote. The initial decrease corresponds to the point where the plasma separation from its initial field line becomes pronounced, thus leading to significant plasma rotation (Eqs. 7 and 26). The slower increase, on the other hand, occurs as the centrifugal force of the rotating plasma becomes much greater than the Lorentz force. It is clear from the graph that the electromagnetic forces are less pronounced for the moderate-$\beta$ case. This is because the currents within the plasma induce a magnetic field that acts to drag the initial flux surface of a plasma element along with it, thereby decreasing the quantity, $\hat{\Psi}_0 - \hat{\Psi}$. The asymptote towards which the work tends reflects the residual energy contained within the plasma rotation. Evidently, this energy is two orders of magnitude less than the energy increase due to thermal forces.

The extent to which the streamlines deviate from the magnetic flux lines can be quantified by considering the separation angle between the magnetic field and velocity vectors at a given point. We will refer to this angle as $\alpha$. Figure 3(e) shows the variation of $\alpha$ along the outermost streamline. The separation angle remains negligibly small until a distance of around five nozzle radii, after which a sharp increase occurs. The increase eventually levels out as the streamline approaches a linear trajectory. It is worthy to note that the separation angle remains small in the region from which a majority of the thermal acceleration occurs, thus justifying the assumptions made in section II.C. Comparing the streamlines of the two flows, we see that the separation angle is greater for the moderate-$\beta$ flow . We can define another angle, $\Delta\alpha$, which is the angle of separation between the velocity vectors of the two flows (i.e. low and moderate-$\beta$ flows). The asymptote of $\Delta\alpha$ indicates a noticeable decrease in the divergence angle for the moderate-$\beta$ plasma.

### III.B. Current Distribution

The azimuthal current density for the moderate-$\beta$ flow is shown in Figure 4(a) along with the flow streamlines (solid black lines) and resulting magnetic flux lines (dashed red lines). Peak values of $\hat{j}_\theta \sim 2 \times 10^{-4}$ are observed along the plume edge around five nozzle radii from the throat. The low-$\beta$ flow shows a similar

trend, however, the peak current density is two orders of magnitude lower than the moderate-$\beta$ flow.

### III.C. Induced Magnetic Field

Figure 4(b) compares the resulting magnetic flux lines (dashed red) to the applied magnetic flux lines (solid blue) for the moderate-$\beta$ flow. It is evident from this figure that the magnetic field lines of the nozzle are stretched along with the flowing plasma as predicted by Arefiev and Breizman.[12,13] However, at a certain point, the streamlines inertially separate from the magnetic field according to Hooper's[10] detachment theory. It thus seems that detachment is a balance between the desire of the plasma to separate from the magnetic field due to its inertia and the tendency of the magnetic field to be pulled along with the plasma. A more detailed analysis of this balance is presented in section III.E.

### III.D. Propulsion Criterion

Before we consider the influence of induced currents on the efficiency of magnetic nozzles, it is imperative to define the nozzle efficiency. Numerous definitions for the efficiency of magnetic nozzles have been reported in the literature,[9,12,19] however, these mainly only examine efficiency losses due to the divergence of the plume and do not take into account the conversion of thermal energy to directed kinetic energy. To this end, we define our nozzle efficiency as

$$\eta_{nozzle} = \frac{P_{thrust}}{P_{in}}, \tag{27}$$

where $P_{thrust}$ is the directed kinetic power of the plume and $P_{in}$ is the power contained within the flow at the throat.

Furthermore, we can express the total nozzle efficiency as a product of efficiencies for two separate processes: acceleration ($\eta_{acc}$) and divergence ($\eta_{div}$). We thus arrive at

$$\eta_{nozzle} = \eta_{acc}\eta_{div}; \qquad \eta_{acc} = \frac{P_{ke}}{P_{in}}; \qquad \eta_{div} = \frac{P_{thrust}}{P_{ke}}; \tag{28}$$

with $P_{ke}$ being the total kinetic power of the flow. Expressions for the input power for a uniform entrance flow and the directed and undirected kinetic power at a given axial position are provided below:

$$P_{in} = \pi r_{p,0}^2 c_{s,0}\left[\left(\frac{1}{2}+\frac{1}{\gamma-1}\right)n_0 M_i c_{s,0}^2 + n_0\epsilon_i^+\right], \tag{29}$$

$$P_{thrust} = 2\pi\int_0^{r_p(z)}(1/2)M_i u_{zi}^3 nrdr, \tag{30}$$

$$P_{ke} = 2\pi\int_0^{r_p(z)}(1/2)M_i u_i^2 u_{zi} nrdr. \tag{31}$$

Assuming only single ionization with ionization energy, $\epsilon_i^+$, and negligible recombination within the expanding plume, we derive an expression for the maximum efficiency assuming all of the thermal energy stored within the plasma is converted into directed kinetic energy. This efficiency is given by

$$\eta_{max} = \left[1+\left(\frac{\gamma-1}{\gamma+1}\right)\hat{u}_{ci}^2\right]^{-1}, \tag{32}$$

where

$$\hat{u}_{ci} = \frac{1}{c_{si,0}}\sqrt{\frac{2\epsilon_i^+}{M_i}} = \sqrt{\frac{2\epsilon_i^+}{k_b T_{e,0}}}, \tag{33}$$

is the normalized critical ionization velocity of the ions. A plot of the maximum efficiency versus $\hat{u}_{ci}$ for three different values of the specific heat ratio, $\gamma$, is presented in Figure 5.

As the normalized critical ionization velocity increases, most of the incoming power is "frozen-in" ionization modes within the plasma. It is thus beneficial to operate at conditions where the sound speed at the throat is much greater than the critical ionization velocity, which is equivalent to a throat temperature much larger than the ionization potential of the gas. Furthermore, the maximum efficiency decreases for an increasing specific heat ratio at a given value of $\hat{u}_{ci}$. This decrease is due to the amount of power contained

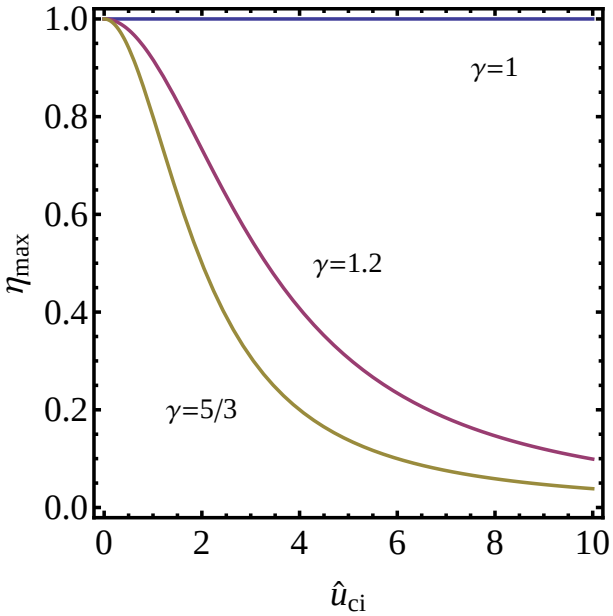


**Figure 5. Maximum nozzle efficiency ($\eta_{max}$) versus normalized critical ionization velocity ($\hat{u}_{ci}$) for three values of the electron specific heat ratio ($\gamma$).**



within the internal modes of the incoming plasma in relation to the power contained within ionization modes. As $\gamma$ decreases, the amount of power contained within these internal modes decreases.

The resulting expressions for the efficiencies as a function of $\hat{z}$ in terms of our normalized variables are

$$\eta_{nozzle} = \frac{2/\hat{r}_{p,0}^2}{1 + 2/(\gamma - 1) + \hat{u}_{ci}^2} \int_0^{\hat{r}_p} (\hat{n}/\hat{n}_0)\, \hat{u}_{zi}^3 \hat{r} d\hat{r}, \tag{34}$$

$$\eta_{acc} = \frac{2/\hat{r}_{p,0}^2}{1 + 2/(\gamma - 1) + \hat{u}_{ci}^2} \int_0^{\hat{r}_p} (\hat{n}/\hat{n}_0)\, \hat{u}_i^2 \hat{u}_{zi} \hat{r} d\hat{r}, \tag{35}$$

$$\eta_{div} = \frac{\int_0^{\hat{r}_p} (\hat{n}/\hat{n}_0)\, \hat{u}_{zi}^3 \hat{r} d\hat{r}}{\int_0^{\hat{r}_p} (\hat{n}/\hat{n}_0)\, \hat{u}_i^2 \hat{u}_{zi} \hat{r} d\hat{r}}, \tag{36}$$

where a quantity in brackets indicates averaging over the cross section at a fixed axial position and the overall values of each efficiency are given by the limit of each expression as $z \to \infty$.

Armed with our efficiency expressions for the different nozzle processes, we may now analyze the effect that induced currents have on magnetic nozzle acceleration and detachment. Applying Equations (32)-(34) to each flow yields the results in figures 6(a)-6(c). The acceleration efficiency is observed to have very little dependence on $\beta_0$, and asymptotes to the maximum value given by Eq.(30). We may then conclude that the induced currents for the values of $\beta_0$ studied in these examples have a negligible effect on the acceleration of the plasma. The divergence efficiency, on the other hand, shows an improvement of four percent for the flow with significant induced currents compared to that without. This improvement is the result of the ability of the moderate-$\beta$ plasma to stretch the field lines along the flow. The result is an increase in the total efficiency from 62% to 65% when going from the low-$\beta$ to moderate-$\beta$ flows - a trend we expect to continue with rising $\beta_0$.

Finally, it is possible to calculate the thrust and specific impulse of the flow at each axial position. Normalizing each parameter with their value at the nozzle throat yields

$$\hat{Th} = \frac{2}{\hat{r}_{p,0}^2} \int_0^{\hat{r}_p} (\hat{n}/\hat{n}_0)\, \hat{u}_{zi}^2 \hat{r} d\hat{r}, \tag{37}$$

$$\hat{I}_{sp} = \frac{2}{\hat{r}^2} \int_0^{\hat{r}_p} \hat{u}_{zi} \hat{r} d\hat{r}, \tag{38}$$

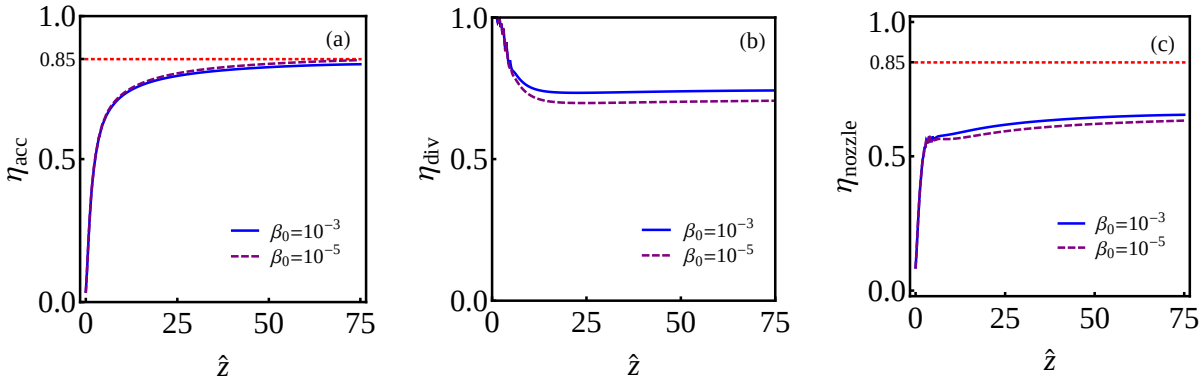


**Figure 6. Evolution of the various efficiencies for $\beta_0 = 10^{-5}$ (dashed) and $\beta_0 = 10^{-3}$ (solid) at each axial position in the flow. (a) Acceleration efficiency, (b) divergence efficiency, (c) nozzle efficiency. Red dotted line denotes the maximum possible efficiency as obtained from Eq. 32.**

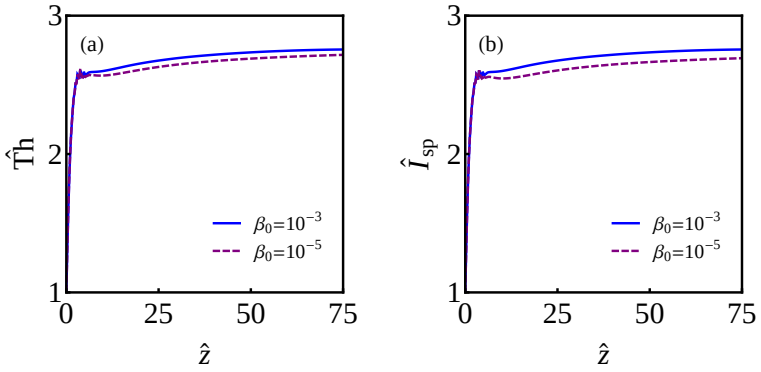


**Figure 7. Evolution of (a) thrust and (b) specific impulse at each axial position in the flow for $\beta_0 = 10^{-5}$ (dashed) and $\beta_0 = 10^{-3}$ (solid).**

where the overall value of each propulsion parameter is given by the above expression as $z \to \infty$. Figures 7(a)-7(b) show that the resulting thrust and specific impulse of each flow asymptote to around 2.8 times their value at the throat, with a small increase in each quantity for the more efficient moderate-$\beta$ flow.

### III.E. Detachment Analysis

The physical mechanism by which plasma detaches from a magnetic nozzle is still open for debate. Our analysis indicates detachment occurs via inertial separation for both flows in consideration. The influence of induced currents is to stretch the magnetic field along the flow, however, the limit suggested by Arefiev and Breizman of the magnetic field being stretched to infinity was not observed. Rather, the magnetic field was stretched by the flow until a certain point where the flow detached inertially. To analyze this phenomenon, we look at electron magnetization and the evolution of $\beta$ within the plume.

The extent to which electrons are demagnetized may be given by the ratio of the electron Larmor radius to the scale length of magnetic variation. Defining this parameter as $\xi_{demag}$, we may write

$$\xi_{demag} = r_{L,e}\frac{|\vec{\nabla}B|}{B}, \tag{39}$$

where a value of $\xi_{demag} << 1$ indicates strongly magnetized electrons.

Figure 8 shows the variation of $\xi_{demag}$ along the outermost streamline for both flows. In each case, $\xi_{demag}$ increases beyond one at nearly two nozzle radii from the throat. Recalling from Figure 3(f) that a sharp increase in the separation angle was observed around five nozzle radii, we conclude that detachment occurs

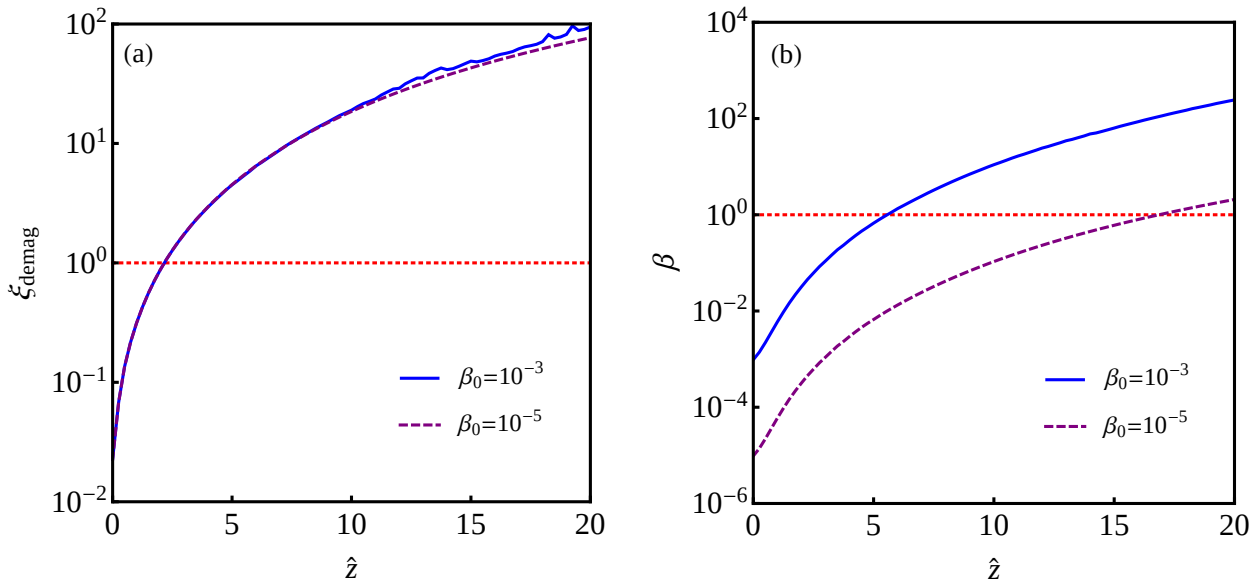


**Figure 8. Axial variation of (a) electron magnetization strength and (b) plasma $\beta$ along the streamline corresponding to the plume boundary ($\hat{r} = \hat{r}_p$) for $\beta_0 = 10^{-5}$ (dashed) and $\beta_0 = 10^{-3}$ (solid).. The electron magnetization strength is on the order of unity at the point of inertial separation ($\hat{z} \approx 5$). For induced currents to influence detachment, $\beta$ at the point of separation also needs to be of order unity.**

due to the effective demagnetization of the electrons. As an electron-ion pair accelerates through the nozzle, the small Larmor radius of the electron ties it to its initial magnetic field line. The ion, having a larger Larmor radius, can wander away from the field line due to its inertia, however, the ambipolar electric field between the particles ties the ion to the electron. If the effective inertia holding the electron to the magnetic field line is greater than the ion inertia, the pair of particles will remain magnetized (large G). However, as the electron Larmor radius increases (small G), the electrons are able to wander away from the magnetic field line, and the inertia of the ions dominates the resulting flow.

The question thus arises: when do induced magnetic fields alter the above detachment scenario? To address this question we consider the variation of $\beta$ along the streamline coincident with the edge of the flow. A plot of $\beta$ versus axial distance along this streamline is presented in Figure 8(b). It is clear from this figure that the axial distance at which $\beta$ increases above unity is strongly dependent on $\beta_0$. The ability of the flow to alter the applied magnetic field lines requires $\beta \sim 1$. Therefore, it is understandable that the induced magnetic fields of the low-$\beta$ flow have no influence over the expansion of the plasma because the point where $\beta$ approaches unity ($\hat{z} \approx 15$) is well downstream the point of inertial detachment ($\hat{z} \approx 5$). The point at which $\beta$ approaches unity for the moderate-$\beta$ flow approximately coincides with the point of inertial detachment, therefore, it is understandable that induced magnetic fields play an important role in the detachment of this flow.

In general, the trends presented in figures 8(a)-(b) depend on the values of G, $\beta_0$, and $\hat{r}_{p,0}$ specified at the nozzle entrance, which in turn are dependent upon the characteristics of the incoming flow. If G is increased, the point at which inertial separation of the flow occurs is pushed downstream. The divergence of the flow at this point is strongly dependent upon $\hat{r}_{p,0}$ as it determines how divergent the magnetic field is at the point of separation. However, the plasma is not guaranteed to reach the separation point before it begins the wrap around the magnetic field, which would lead to thrust losses and possible spacecraft damage. This scenario may be avoided if $\beta_0$ is large enough to stretch the field along with the flow. A thorough characterization of the effect of these three variables on plasma detachment is outside the scope of this paper, however, future work is aimed at quantifying this complex rapport.

## IV. Conclusion

We have presented a model for the acceleration and detachment of a two-fluid plasma flow through a magnetic nozzle. The model considers cold ions and hot electrons. Ion acceleration occurs as the electron thermal energy is converted into ion kinetic energy by an ambipolar electric field. A quasi-one-dimensional expression for the pressure is derived that allows us to solve for the flow dynamics in a Lagrangian reference frame. An iterative procedure is then employed to solve for a magnetic field consistent with the induced currents within the flow. Using this model, we examined the influence of induced currents on the plasma expansion using a low-$\beta$ flow and a moderate-$\beta$ flow. Analysis of a high-$\beta$ flow requires an alternative iteration scheme and will be the subject of a future study.

Induced currents were observed to have a negligible influence on the thermal acceleration of the plasma for both flows in consideration. The divergence of the plasma due to electromagnetic forces, on the other hand, decreased by around three degrees for the moderate-$\beta$ case. This decrease is attributed to the stretching of the magnetic field along with the flow, resulting in a less divergent field at the point of inertial detachment.

A definition of the nozzle efficiency was presented as the ratio of the directed kinetic power of the flow to the total power of the flow at the nozzle entrance. We derived an expression for the maximum nozzle efficiency that indicates high efficiencies require operation in which the speed of sound at the nozzle throat is on the order of the critical ionization velocity of the ions. This requirement ensures that "frozen-flow" losses due to ionization of the propellant are a small fraction of the directed kinetic energy. Furthermore, we considered the contribution of an acceleration efficiency and a divergence efficiency to the total nozzle efficiency for both flows. It was determined that induced currents do not influence the efficiency by which thermal energy is converted into kinetic energy. The fraction of the kinetic energy that is directed along the thrust axis increases with the magnitude of the induced currents, however, as the induced magnetic fields lead to a decreased plume divergence.

Finally, the implications for plasma detachment were analyzed by considering the variation of the electron magnetization strength and the plasma beta along the plume boundary. We observed that the plasma detaches by inertial separation for both flows in consideration. Furthermore, the point of detachment occurs when the electron Larmor radius is on the order of the scale length of magnetic variation. It is thus concluded that inertial separation as the electrons become demagnetized is the predominant detachment mechanism by which the plasma separates from the magnetic field. We also found that, if induced currents are to influence the flow, the local value of the plasma $\beta$ must be of order unity at the point of inertial separation. We conclude that the divergence efficiency associated with plasma detachment is ultimately dependent upon three dimensionless variables associated with the incoming flow: the inertial detachment parameter, $G$, the ratio of the flow energy density to the magnetic field energy density, $\beta_0$, and the ratio of the plasma radius to the nozzle radius, $\hat{r}_{p,0}$.



## Acknowledgments

This work is supported by the Air Force Office of Scientific Research through the National Defense Science and Engineering Graduate Fellowship. Further support comes from the Program in Plasma Science and Technology at the Princeton Plasma Physics Laboratory.

## References

[1]Cohen, S., Ferraro, N., Scime, E., Miah, M., Stange, S., Siefert, N., and Boivin, R., "On collisionless ion and electron populations in the magnetic nozzle experiment (MNX)," *IEEE Transactions on Plasma Science*, Vol. 34, No. 3, June 2006, pp. 792–803.

[2]Arefiev, A. V. and Breizman, B. N., "Theoretical components of the VASIMR plasma propulsion concept," *Physics of Plasmas*, Vol. 11, No. 5, 2004, pp. 2942.

[3]Andersen, S., Jensen, V., Nielsen, P., and D'Angelo, N., "Continuous supersonic plasma wind tunnel," *Physics Letters A*, Vol. 27, No. 8, 1968, pp. 527–528.

[4]Moses Jr, R., Gerwin, R., and Schoenberg, K., "Resistive plasma detachment in nozzle based coaxial thrusters," *AIP Conference Proceedings*, Vol. 246, 1992, p. 1293.

[5]Cohen, S. and Paluszek, M. A., "The Grand Challenge: A New Plasma Thruster," 1998.

[6]Kuriki, K. and Okada, O., "Experimental Study of a Plasma Flow in a Magnetic Nozzle," *Physics of Fluids*, Vol. 13, 1970, pp. 2262.

[7]Dimov, G. I. and Taskaev, S. Y., "Simulation of a supersonic plasma jet with recombination in a magnetic nozzle," *27th EPS Conference on Contr. Fusion and Plasma Phys.*, Vol. 24, 2000, pp. 464–467.

[8]Cohen, S. a., Siefert, N. S., Stange, S., Boivin, R. F., Scime, E. E., and Levinton, F. M., "Ion acceleration in plasmas emerging from a helicon-heated magnetic-mirror device," *Physics of Plasmas*, Vol. 10, No. 6, 2003, pp. 2593.

[9]Kosmahl, H. G., "Three-dimensional plasma acceleration through axisymmetric diverging magnetic fields based on dipole moment approximation," *Nasa Technical Report*, 1967.

[10]Hooper, E., "Plasma detachment from a magnetic nozzle," *Journal of Propulsion and Power*, Vol. 9, No. 5, 1993, pp. 757–763.

[11]Schmit, P. F. and Fisch, N. J., "Magnetic detachment and plume control in escaping magnetized plasma," *Journal of Plasma Physics*, Vol. 75, No. 03, Nov. 2008, pp. 359.

[12]Arefiev, A. V. and Breizman, B. N., "Magnetohydrodynamic scenario of plasma detachment in a magnetic nozzle," *Physics of Plasmas*, Vol. 12, No. 4, 2005, pp. 043504.

[13]Breizman, B. N., Tushentsov, M. R., and Arefiev, a. V., "Magnetic nozzle and plasma detachment model for a steady-state flow," *Physics of Plasmas*, Vol. 15, No. 5, 2008, pp. 057103.

[14]Little, J. M. and Choueiri, E. Y., "Divergence of a Propulsive Plasma Flow Expanding through a Magnetic Nozzle," *31st International Electric Propulsion Conference*, Ann Arbor, Michigan, 2009.

[15]Deline, C. a., Bengtson, R. D., Breizman, B. N., Tushentsov, M. R., Jones, J. E., Chavers, D. G., Dobson, C. C., and Schuettpelz, B. M., "Plume detachment from a magnetic nozzle," *Physics of Plasmas*, Vol. 16, No. 3, 2009, pp. 033502.

[16]Jackson, J. D., *Classical Electrodynamics*, John Wiley & Sons, Inc., New York, 1962.

[17]Ilin, A., Chang-Diaz, F., Squire, J., Tarditi, A., Breizman, B., and Carter, M., "Simulations of Plasma Detachment in VASIMR," *40th AIAA Aerospace Sceinces Meeting \& Exhibit, Reno, NV*, No. January, 2002.

[18]Winglee, R., Ziemba, T., Giersch, L., Prager, J., Carscadden, J., and Roberson, B. R., "Simulation and laboratory validation of magnetic nozzle effects for the high power helicon thruster," *Physics of Plasmas*, Vol. 14, No. 6, 2007, pp. 063501.

[19]Ahedo, E. and Merino, M., "Acceleration of a focused plasma jet in a divergent magnetic nozzle," *31st International Electric Propulsion Conference*, 2009, pp. 1–10.

[20]Martínez, M. M. and Ahedo, E., "Two-Dimensional Magnetic Nozzle Acceleration of a Two-Electron Component Plasma pansion," *Space Propulsion Conference 2010*, 2010.

[21]Jardin, S., *Computational Methods in Plasma Physics*, CRC Press, 1st ed., 2010.

[22]Batishchev, O. V., "Minihelicon Plasma Thruster," *IEEE Transactions on Plasma Science*, Vol. 37, No. 8, Aug. 2009, pp. 1563–1571.